Distinct Regulatory Roles of Lymphocyte Costimulatory Pathways on T Helper Type 2–Mediated Autoimmune Disease

By Luigi Biancone,* Giuseppe Andres,* Hannah Ahn,* Alice Lim,* Charlotte Dai,* Randolph Noelle,‡ Hideo Yagita,§ Cesare De Martino,‖ and Ivan Stamenkovic*

*From the *Department of Pathology, Harvard Medical School, and Pathology Research, Massachusetts General Hospital, Charlestown Navy Yard, Boston, MA 02129; ‡Department of Microbiology, Dartmouth Medical School, Lebanon, New Hampshire 03756; §Department of Immunology, Juntendo University School of Medicine, Bunkyo-ku, Tokyo 113, Japan; and ‖Istituto Dermatologico S. Gallicano, Rome, Italy 0041*

Summary

We assessed the role of CD40–CD40L, cytotoxic T lymphocyte (CTL)A4/CD28-B7s, and CD2–CD48/CD58 lymphocyte costimulatory pathways in the development of mercury chloride ($HgCl_2$)–induced autoimmune disease in mice, which is believed to be mediated by T helper (Th) subset Th2. Inhibition of CD40–CD40L and CTLA4/CD28-B7s interactions by anti–CD40L antibody and soluble CTLA4–immunoglobulin (Ig) fusion protein, respectively, abrogated the autoimmune disease without affecting interleukin 4 (IL-4) production, showing the importance of physical contact between T and B lymphocytes in the Th2-mediated process. In contrast, two anti–CD2 antibodies that have been shown to induce immunosuppression of Th1-mediated events exacerbated the autoantibody response and augmented IgG1, IgE, and IL-4 production, transforming a mild mesangial glomerulopathy into a severe systemic immune complex disease. These observations demonstrate that manipulation of lymphocyte accessory counterreceptor interactions may affect the course of Th2-associated autoimmune disease and suggest that signals resulting from CD2 engagement may play an essential role in the regulation of the Th1-Th2 effector equilibrium.

The effector mechanisms of the immune response are selected by preferential activation of distinct Th subsets, Th1 and Th2, which express and respond to distinct groups of cytokines. Recent evidence suggests that signals generated by specific cell surface counterreceptors that mediate T cell–APC interactions may be important in promoting T cell differentiation to the Th1 or Th2 phenotype (1, 2). Several cell surface counterreceptors also provide costimulatory axes that are implicated in the regulation of T and APC/B cell responses as a result of cognate interaction. In particular, CD40–CD40L, CD28/CTLA4-B7s, and CD2–CD48/CD58 counterreceptors transduce critical signals for the regulation of lymphocyte activation in response to antigenic stimulation.

The receptor–ligand pair composed of the B cell–associated receptor CD40 and its T cell ligand CD40L/gp39 has been shown to play a key role in the regulation of T cell–dependent B cell proliferation, antibody production, and isotype switching (3). The CTLA4/CD28-B7s pathways also trigger B cell responses (4), but in addition transduce essential costimulatory signals for T cell activation (5). CD28 costimulation is important for activation and proliferation of both Th1 and Th2 clones (6, 7). The principal CD2 ligand is LFA-3 in humans and CD48 in mice (8), a glycosyl phosphatidylinositol-anchored glycoprotein expressed on most T and B cells. Engagement of CD2 by mAbs as well as by soluble recombinant LFA-3 has been shown to have a costimulatory effect on T cell activation (9). Conversely, a potent immunosuppressive effect of anti-CD2 mAbs has been observed in vivo, and shown to inhibit the Th1-mediated/cytotoxic immune response (10–13).

In this work, we have examined the implication of lymphocyte costimulatory pathways in the development of $HgCl_2$-induced autoimmune disease in SJL mice. In mice, rats, and rabbits, mercury, penicillamine, and gold induce autoimmune responses that have several common features, including the production of anti–basement membrane and antinuclear antibodies, immune complex glomerulonephritis, and upregulation of MHC class II expression on B lymphocytes (14). In addition, these heavy metal–induced disorders present with increased production of IgG1, IgE, IL-4, and IL-10, with a concomitant decrease in IL-2 and IFN-γ production, consistent with preferential activation of Th2 lymphocytes (15). mAbs to IL-4 prevent some dis-

 J. Exp. Med. © The Rockefeller University Press • 0022-1007/96/04/1473/09 $2.00
Volume 183 April 1996 1473–1481

ease manifestations, supporting the hypothesis that murine drug-induced autoimmunity is characterized, and possibly induced, by a Th1–Th2 imbalance (16).

Materials and Methods

Animals and Autoimmune Disease Induction. 8- to 9-wk SJL/J (H-2s) mice were purchased from Jackson Laboratories (Bar Harbor, ME) and injected subcutaneously with 1.6 mg of $HgCl_2$ per kilogram of body weight every third day for 4 wk. The mice were bled 2 and 4 wk after the beginning of the experiments and killed at various intervals of time as described. Six mice were immunized in the hind footpads with ~25 μl of 1 mg/ml chicken OVA emulsified in CFA (Difco Laboratories, Detroit, MI) (17). The mice were killed 3–5 d after footpad injections.

Antibodies and Flow Cytometry. Hamster anti–mouse CD40L (clone MR1) mAb (18), rat anti–mouse CD2 mAbs RM2-1 (19) and 12–15 (10), and hamster anti–mouse CD48 (13) were prepared and purified as previously described. Rat anti–mouse IL-4 mAb 11B11 was purchased from the American Type Culture Collection (ATCC, Rockville, MD); rat anti–mouse IL-10 mAb SXC-1 was a kind gift from Drs. S. Reed and Coffman. For immunohistochemical and flow cytometry studies, the following antibodies were used: rat anti–mouse Thy 1.2, IL-4 (BVD6-24G2), IL-2 (S4B6), IFN-γ (XMG12), CD45R/B220 (RA3-6B2), CD4 (RM4-5), and CD8 (53-6.7) mAbs from PharMingen (San Diego, CA); FITC-conjugated rat anti–mouse IgE mAb from Serotec/Harlan Sprague Dawley (Indianapolis, IN); and FITC–rabbit anti-mouse IgG, IgM, and C3 from Cappel Laboratories, Inc. (West Chester, PA). Purified hamster, human, and rat IgGs (Cappel) were used as controls. FACS® analysis for $Thy1.2^+$ and $CD45R/B220^+$ cells was performed on Ficoll-separated splenocytes.

Immunohistochemistry and Morphology. Kidney, heart, muscle, liver, testes, and spleen from mice injected with $HgCl_2$, subcutaneous tissue from the footpads of mice locally immunized, and tissues from control mice were removed at sacrifice. Tissues were processed for immunofluorescence and electron microscopy as previously described (20). For immunohistochemical analysis, serial 4-μm thick skin and spleen sections were incubated for 60 min at room temperature with biotinylated primary mAbs and revealed by incubation with avidin–biotin horseradish peroxidase complexes (Vectastain Elite ABC; Vector Laboratories, Inc., Burlingame, CA). Peroxidase activity was detected with 3-amino-9-ethylcarbazole. For two-color immunocytochemical analysis, serial sections single-stained for cytokines as described above were double stained with mAbs to T and B cell markers, a secondary biotin-conjugated mAb, and ExtrAvidin–alkaline phosphatase, revealed by 4-chloro-1-naphthol (Sigma Chemical Company, St. Louis, MO). The sections were lightly counterstained with hematoxylin. The amount and extent of fluorescence were semiquantitatively graded on a scale from 0 to 4 (0, absent; +, minimal and focal; ++, moderate and focal; +++, moderate and diffuse; ++++, marked and diffuse).

Measurement of Circulating Mouse Total IgG, IgG1, IgG2a, and IgE by ELISA. In all mice included in the experimental groups, the levels of IgG, IgG1, IgG2a, and IgE were measured on serum samples obtained 0, 15, and 30 d after the beginning of the experiments. 96-well microtiter plates were coated overnight at 4°C with 1 μg/ml goat anti–mouse IgG (Cappel) or rat anti–mouse IgE mAb (Harlan Sprague Dawley). The plates were washed with PBS–0.05% Tween 20 and incubated with PBS–2% skimmed milk for 30 min at room temperature. After two washes, serial 1:50–1:500 dilutions of mouse sera (100 μl/well) were added. After an overnight incubation at 4°C, the plates were washed and exposed for 4 h to alkaline phosphatase–conjugated goat anti–mouse IgG (Sigma), or rat anti–mouse IgG1, IgG2a, or IgE (PharMingen) diluted 1:4,000. After washing, *p*-nitrophenyl phosphate (Sigma) was added, and the colorimetric reaction was read at 405 nm.

Measurement of Antinucleolar Antibodies by Immunofluorescence. The titers of anti-nucleolar antibodies (ANolAs)[1] were measured by indirect immunofluorescence using the HepG-2 human hepatoma cell line (ATCC). HepG-2 cells were cultured in 20-mm (diameter) plastic dishes in RPMI 1640 supplemented with 10% FCS. Subconfluent cells were fixed in a 4% formaldehyde/PBS solution, washed twice with PBS, and permeabilized with 0.1% Triton X-100 in PBS for 10 min. After three washes with PBS, cells were incubated for 1 h at 37°C with serial dilutions of the mouse sera, washed, and incubated with affinity-purified, FITC-conjugated rabbit anti–mouse IgG (Cappel), diluted 1:500, for 45 min at 37°C. The titers were expressed as reciprocal value of the highest serum dilution that gave an unequivocal positive reaction.

Development and Production of Soluble Recombinant Fusion Proteins. Soluble receptor globulins were developed by genetic fusion of sequences encoding the extracellular region of murine CTLA4 to human IgG1 Fc genomic DNA sequences (21). Synthetic oligonucleotide primers complementary to the 5′ and 3′ extremities of the nucleotide sequence encoding the extracellular domain of murine CTLA4, containing, respectively, an XhoI and a BamHI restriction site, were used to PCR-amplify mouse CTLA4 from cDNA derived from Con A–stimulated CTLL-2 murine cytotoxic T cells (ATCC). Nucleotide sequences of the primers were the following: forward, 5′-CAC GGG CTC GAG ATG GCT TGT CTT GGA CTC CGG AGG-3′; reverse, 5′-CAC GGG ATC CCA AAG GAG GAA GTC AGA ATC CGG GCA-3′. PCR amplification was performed as described (21). Amplified cDNA was subjected to XhoI–BamHI digestion and ligated to XhoI–BamHI-cut human IgG1 expression vector. Plasmids containing sequences encoding CTLA4 receptorglobulin were cotransfected with a pSVNeo vector into Chinese hamster ovary (CHO) cells (ATCC) by electroporation at 250 V/960 μF using a gene pulser (Bio-Rad Labs., Richmond, CA). Transfected CHO cells were selected for G418 (GIBCO BRL, Inc., Gaithersburg, MD) resistance. Resistant CHO clones were screened for the production of CTLA4 Rg by ELISA detection of the human IgG Fc domain in the supernatants. Soluble fusion proteins were purified from supernatants on protein A–Sepharose, as previously described (21). A soluble CD8 Rg fusion protein (21) was used as a control.

Statistics. Statistical analysis, when applicable, was performed with Statview IV software (Abacus Concepts, Berkeley, CA) on a Macintosh SE computer (Apple Computer, Inc., Cupertino, CA). Differences between groups were compared with one-way analysis of variance and unpaired *t* test.

Results

$HgCl_2$-induced Glomerular and Vascular Lesions. 13 groups of six to seven mice each were used (Table 1). Five control

[1] *Abbreviations used in this paper:* ANolA, anti-nucleolar antibody; CHO, Chinese hamster ovary; PALS, periarteriolar lymphoid sheath.

groups were established, one of which received no $HgCl_2$. The other four control groups were treated with $HgCl_2$ alone or $HgCl_2$ along with human and/or rodent IgG, or human CD8–Ig fusion protein (CD8Rg), at the same frequency and dosage as the test groups (Table 1). In each of the five test groups, animals were treated with $HgCl_2$ and received CTLA4 Rg alone, anti–CD40L mAb MR1 alone, a combination of CTLA4 Rg and MR1, anti–CD2 mAb RM2-1, anti–CD2 mAb 12-15, anti–CD48 mAb HM-48, or anti–CD2 mAb 12-15 in combination with either anti–IL-4 (22) or anti–IL-10 mAb (23) (Table 1). 2 and 4 wk after the beginning of the experiments, mice injected with $HgCl_2$ (group II) or with $HgCl_2$ and control reagents (groups III–V) had a significant increase in total serum IgG (data not shown), IgG1 (Fig. 1 *A*), and, to a lesser extent, IgG2a (Fig. 1 *B*) with respect to naive mice (group I). IgE levels were augmented 60- and 34-fold at 2 and 4 wk, respectively (Fig. 1 *C*). At 4 wk, all mice injected with $HgCl_2$ and IgG or CD8 Rg had developed ANolAs (Fig. 2).

Spleen tissue sections from mice killed 1, 3, 6, or 12 h and 2, 5, 15, or 30 d after the beginning of $HgCl_2$ injection were subjected to immunocytochemical analysis for IFN-γ, IL-2, and IL-4 expression. As a positive control for IFN-γ and IL-2 expression, skin and spleen tissue sections of C57BL/10 mice, immunized 7 d previously in the footpad with ovalbumin in CFA, were examined. Consistent with observations by others (17), IFN-γ– and IL-2–producing cells were identified around dermal vessels (Fig. 3 *a*) and in the red pulp of the spleen (Fig. 3 *c*), respectively. In contrast, IFN-γ (Fig. 3 *b*) and IL-2 (Fig. 3 *d*) expression was not detectable in the spleens of mice injected with $HgCl_2$ during the entire period of observation. IL-4, on the other hand, was visualized in the periarteriolar lymphoid sheaths (PALSs) and in the areas in which PALSs merge with the follicular mantle as early as 1 h after the first injection of $HgCl_2$. After 2 d, IL-4 was detected on the surface of B cells in the mantle and marginal zones of lymphoid follicles. Between 15 and 30 d after injection, a diffuse staining pat-

Table 1. *Experimental Design*

Group	Number of mice	$HgCl_2$	Treatment
I	7	−	None
II	6	+	None
III	6	+	Human IgG + Hamster IgG
IV	3	+	CD8 Rg
V	6	+	Rat IgG
VI	6	+	CTLA-4 Rg
VII	6	+	Anti-CD40L mAb (MR1)
VIII	6	+	CTLA-4 Rg + Anti-CD40L mAb (MR1)
IX	6	+	Anti-CD2 mAb (RM2-1)
X	6	+	Anti-CD2 mAb (12-15)
XI	6	+	Anti-CD48 mAb (HM48-1)
XII	6	+	Anti-CD2 mAb (12-15) + Anti-IL4 mAb (11B11)
XIII	6	+	Anti-CD2 mAb (12-15) + Anti-IL10 mAb (SXC-1)

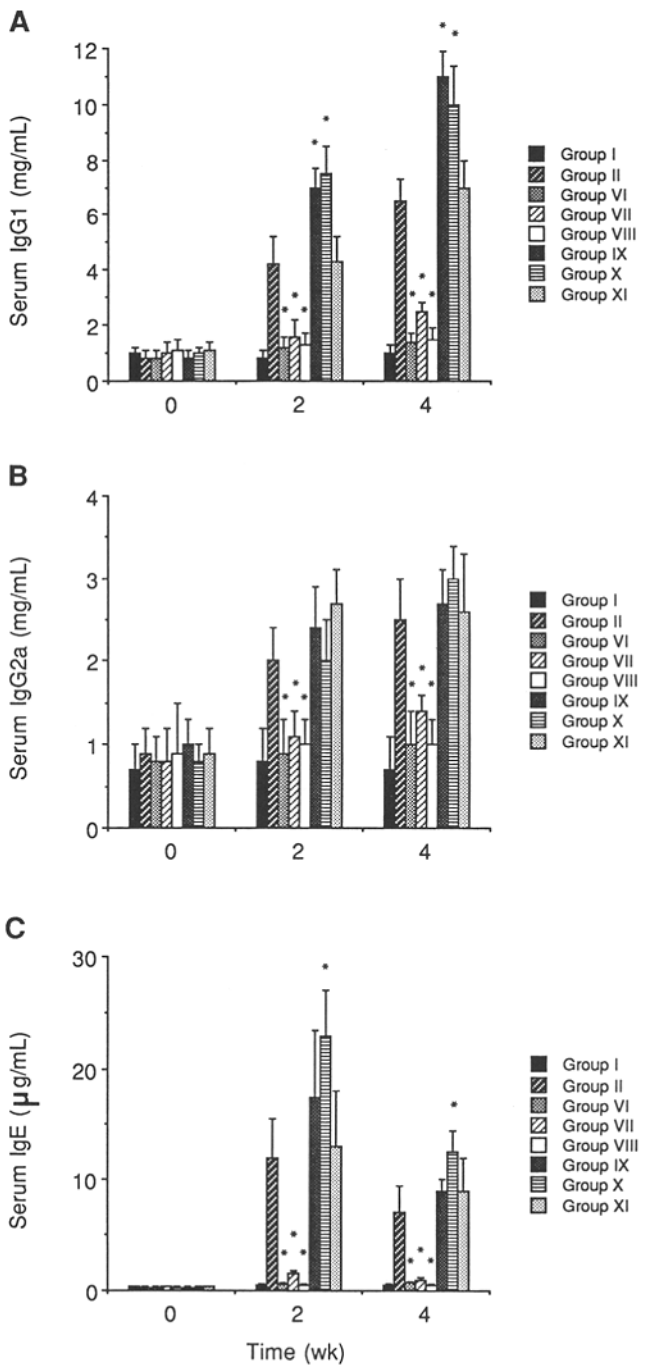

Figure 1. Serum levels of IgG1 (*A*), IgG2a (*B*), and IgE (*C*) detected by ELISA at 2 and 4 wk after the beginning of the experiments. Data are shown as means ± SD. Control groups II–V showed comparable results. Statistical analysis was performed between group II and groups VI–XI (*$P < 0.05$).

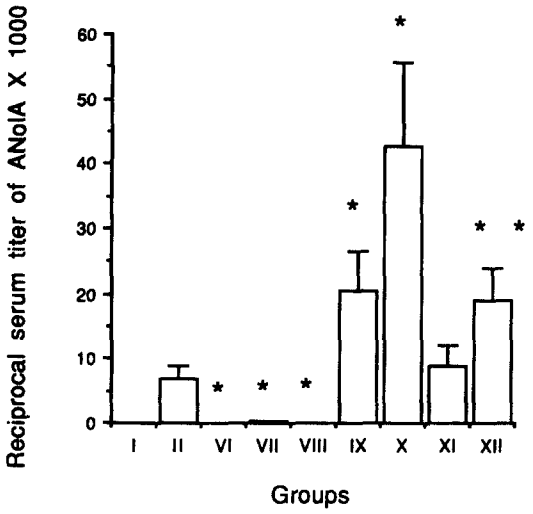

Figure 2. Levels of circulating ANolA IgG at 4 wk measured by indirect immunofluorescence using Hep-G2 cells. At day 0 and at 2 wk, ANolAs were undetectable. In group II, ANolA levels were comparable to those of groups III–V. Data are expressed as the mean ± SD. Statistical analysis was performed for groups VI–XI, with group II values as the baseline ($^*P < 0.05$).

tern for IL-4 was observed in PALSs and in the marginal zones. The number of Thy1.2$^+$, CD4$^+$ cells, and plasma cells progressively increased in the red pulp during the observation period; the germinal centers and the number of CD45R/B220$^+$ cells in the follicular mantles were also augmented. No appreciable variation in number and distribution of CD8$^+$ cells was observed.

Untreated mice (group I) had minimal focal and segmental deposition of IgG in the glomerular mesangium, but not in the vasculature (Fig. 4 *a*). Mice injected with $HgCl_2$ alone (group II) or $HgCl_2$ and control reagents (groups III–V) presented with abundant mesangial deposition of IgG in all glomeruli (Fig. 4 *b*). In the capillaries of lung, liver, and testis, deposits of IgG were absent or minimal, and focal but granular deposits of IgG were present in the walls of large vessels, especially arteries, in all organs.

CTLA4 Rg and Anti–CD40L mAb MR1 Prevent the Development of HgCl2-mediated Glomerular and Vascular Lesions. Animals treated with $HgCl_2$ and injected with 300 μg of CTLA4 Rg on days 0, 5, and 15 (group VI) revealed normal serum levels of total IgG (data not shown), IgG1, IgG2a, and IgE (Fig. 1) and undetectable levels of ANolA (Fig. 2) at 2 and 4 wk. In mice injected at the same time points with 250 μg of anti–CD40L mAb MR1 (group VII), serum IgG levels were normal at 2 wk and increased at 4 wk, although to a significantly lesser degree than in group II animals. Similarly, serum IgE levels were reduced at 2 and 4 wk with respect to those in group II mice. ANolAs were detectable, at a low titer, in one mouse only. Treatment with a combination of CTLA4 Rg and MR1 (group VIII) resulted in normal serum total IgG, IgG1, IgG2a, and IgE levels and absence of detectable ANolAs during the entire duration of the study (Figs. 1 and 2).

Splenocyte expression of IL-4, IL-2, and IFN-γ was not significantly different from that of group II animal counterparts. Similarly, T and B cell populations were comparable to those in spleens of group I and II mice, as demonstrated by days 15 and 30 flow cytometry analysis of Thy1.2$^+$ and CD45R/B220$^+$ splenocytes (data not shown). No significant variation in the number of PBL was observed (data not shown), indicating that the effects of CTLA4 Rg and anti-CD40L mAbs were not due to lysis of target cells but rather to abrogation of specific intercellular signals. None of the animals in these three groups had vascular wall IgG deposits, and glomerular mesangial deposits were minimal or absent (Fig. 4, *a*, *c*, and *d*).

Engagement of CD2 Induces an Unusually Severe Systemic Immune Complex Disease in $HgCl_2$-treated Mice. In mice injected at days 0, 5, and 15 with $HgCl_2$ and 200 μg of either RM2-1 (group IX) or 12-15 anti-CD2 mAbs (group X), serum IgG, IgG1, IgE, and ANolAs but not IgG2a levels were significantly augmented, in comparison with those in animals treated with $HgCl_2$ alone (Figs. 1 and 2). Immunohistochemical analysis of the spleens of these animals showed an absence of detectable IFN-γ and IL-2, in contrast with markedly enhanced IL-4 expression (visible 6 h after $HgCl_2$/anti-CD2 mAb injection) in comparison with that observed in mice treated with $HgCl_2$ only (Fig. 3, *g* and *h*).

Abundant, diffuse granular deposits of IgG were observed by immunofluorescence in the mesangium of all glomeruli and in the basal part of proximal, distal, and collecting tubules (Fig. 5 *a*). Similar deposition of IgG was detected in the alveolar (Fig. 5 *c*) and cardiac (Fig. 5 *d*) capillaries, sinusoids, basement membranes of seminiferous tubules, and arteries and veins of all of the organs examined. Moreover, mouse IgG was found in cardiac myofibrils and along the Z lines (Fig. 5 *d* and its inset). By electron microscopy, dense deposits were seen in the mesangial matrix (Fig. 5 *b*) and along the basement membranes and matrix between smooth muscle cells in the arteries (data not shown). Anti-CD48 mAbs did not alter the development of the disease as assessed by the serological and immunohistological findings (data not shown).

To determine whether the effect on disease development of anti-CD2 antibodies was primarily due to Th2 cell–derived cytokines, IL-4 and IL-10, two groups of mice were injected with anti-CD2 mAb 12-15 on days 0, 5, and 15, together with either 200 μg per injection of anti–IL-4 mAb 11B11 (22) or anti–IL-10 mAb SXC-1 (23). Anti–IL-4 mAb partially reduced the ANolA titers in all of the animals (Fig. 2) and IgG deposits in renal and extrarenal tissues in two out of six mice (data not shown). The total IgG and IgE titers remained comparable to those in animals treated with mAb 12-15 alone. Anti–IL-10 mAb had no effect on any of the anti-CD2 mAb-induced disease parameters (data not shown).

Discussion

In the present study, we have shown that an imbalance between Th1 and Th2 population cytokine production is

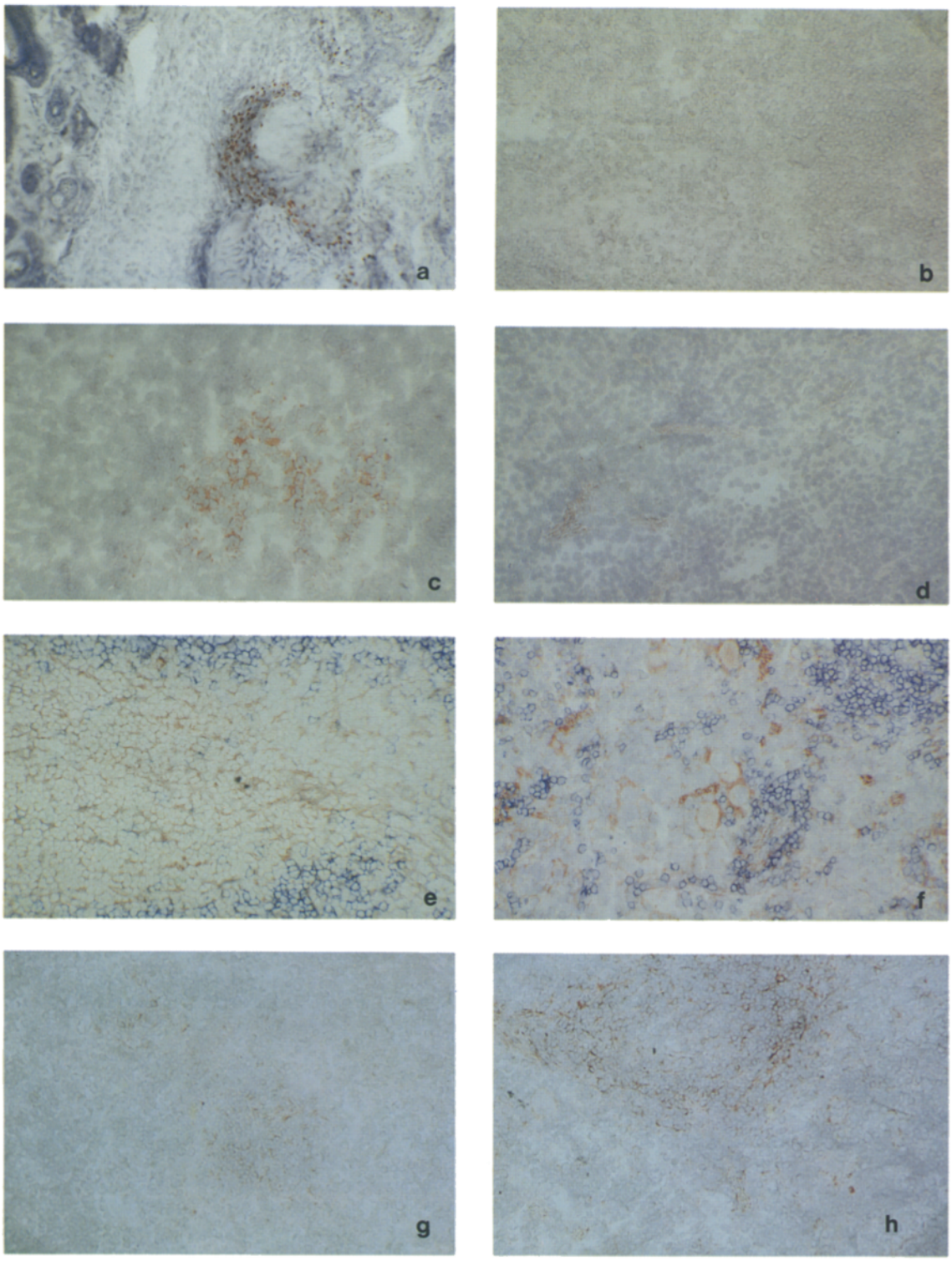

Figure 3. Cytokine production in the skin and the spleen assessed by in situ immunocytochemistry. (*a*) IFN-γ production by cells (*brown color*) infiltrating the skin of a mouse 7 d after local immunization with OVA in CFA. (*b*) Absence of IFN-γ^+ cells in the spleen of a mouse 30 d after the beginning of injections of $HgCl_2$. (*c*) IL-2^+ cells (*light brown*) in the spleen of a mouse 7 d after immunization with OVA, as described in (*a*). (*d*) Absence of IL-2^+ cells in the spleen of a mouse 30 d after injection of $HgCl_2$. (*e*) IL-4^+ cells (*light brown*) in the PALS region 6 h after injection of $HgCl_2$; at the periphery of PALSs, IL-4 overlaps with CD45R/B220^+ cells (*blue*). (*f*) IL-4^+ (*brown*) and CD45R/B220^+ (blue) cells in the red pulp of a mouse 30 d after injection of $HgCl_2$. (*g*) IL-4^+ splenocytes 6 h after injection of $HgCl_2$. (*h*) IL-4^+ splenocytes 6 h after injection of $HgCl_2$ and anti-CD2 mAb 12-15. ×300 (*a*, *b*, *d*, *g*, and *h*); ×400 (*c* and *e*).

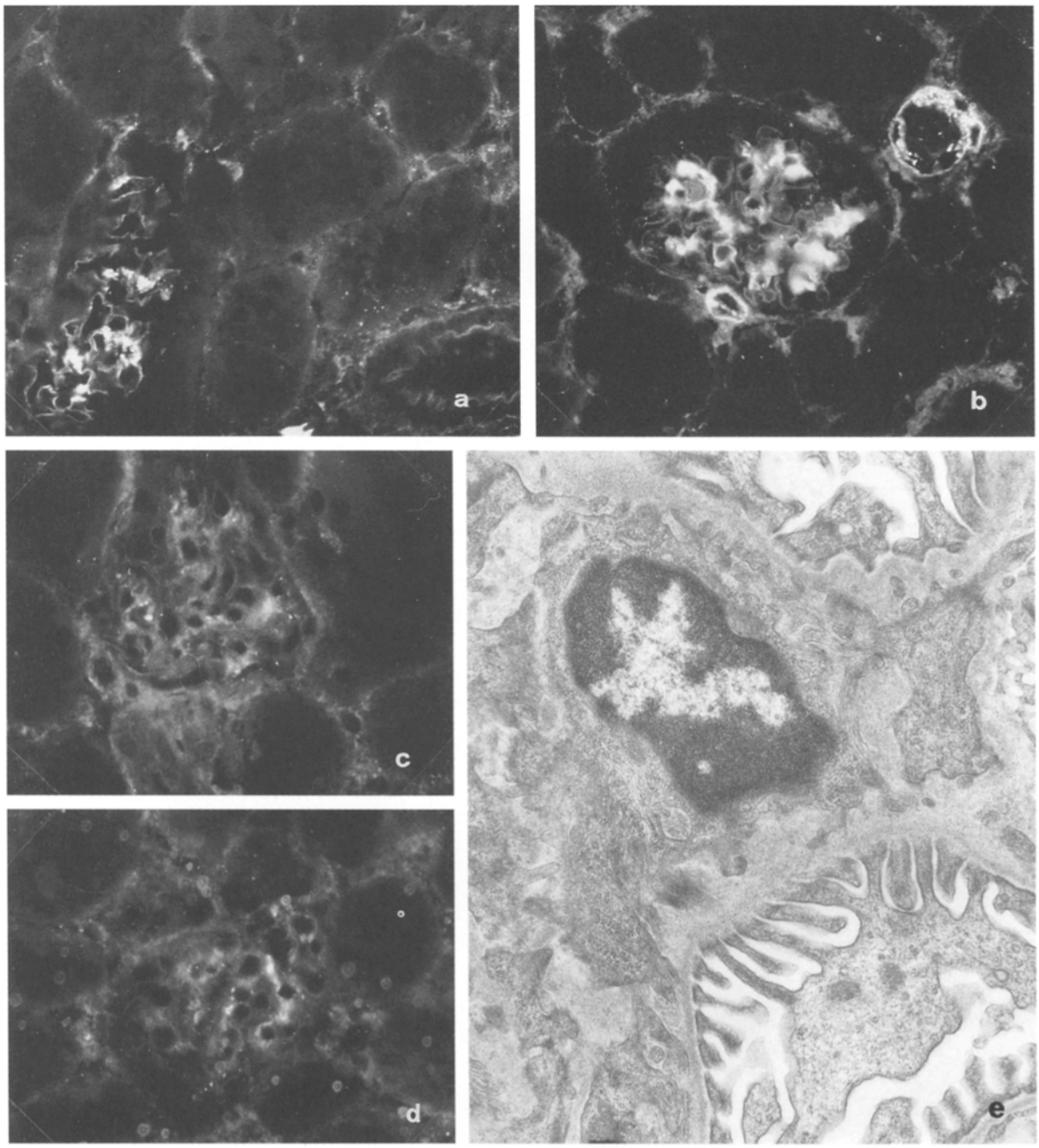

Figure 4. Immunofluorescence microscopy of glomerular and vascular lesions. (*a*) Minimal and focal deposition of mouse IgG (+) in mesangium of a naive SJL mouse (group I). IgGs are absent in the tubules and in the walls of an artery (*lower right*). (*b*) Renal tissues from an SJL mouse injected with $HgCl_2$ and killed at day 30 (group II). Moderate deposition of IgG (++) in the mesangium and in the walls of arterioles. Minimal and segmental deposition of IgG (+) in the mesangium of SJL mouse injected with (*c*) $HgCl_2$ and CTLA4 Rg (group VI), and (*d*) $HgCl_2$ and MR1 mAb (group VII). (*e*) By electron microscopy, the mesangium of a mouse from group VII appears normal. ×400 (*a–d*); ×14,000 (*e*).

associated with $HgCl_2$-induced disease and that soluble CTLA4 Rg and anti-CD40L mAb, alone or in combination, prevent the development of $HgCl_2$-induced autoimmune glomerular and vascular lesions in mice. In contrast, two different anti-CD2 antibodies that have been shown to exert an inhibitory effect on lymphocyte activation in vitro (8, 24) and in vivo (10, 11, 25) markedly enhanced the autoimmune manifestations and induced an unusually severe systemic immune complex disease.

The inhibition of the disease by anti-CD40L antibody and CTLA4 Rg treatment underscores the importance of physical T cell–B cell interaction and that of the CD40–CD40L and CTLA4/CD28–B7.1/B7.2 pathways in the generation of a Th2-mediated autoimmune process. Inter-

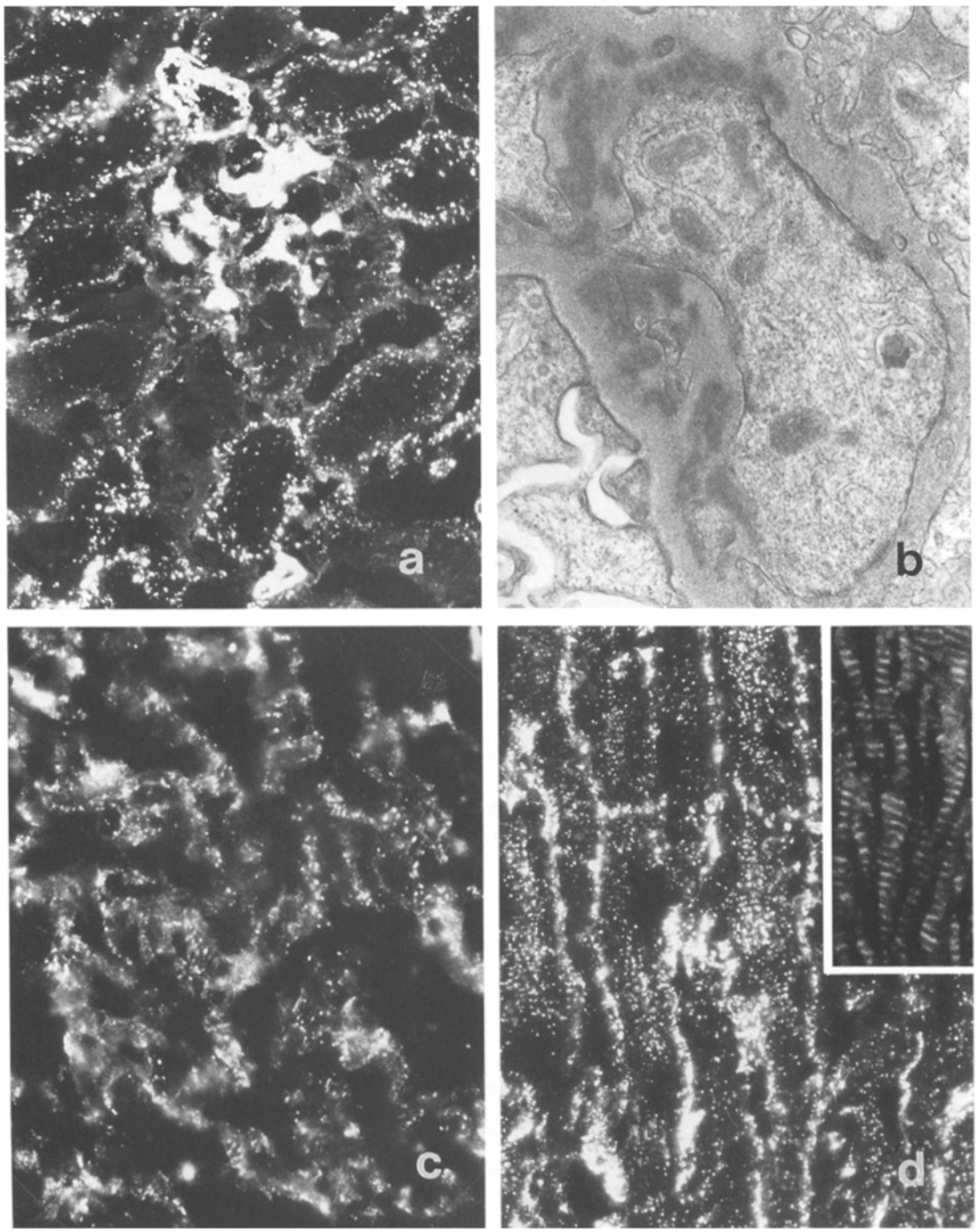

Figure 5. Immunofluorescence and electron microscopy of tissues from mice injected with $HgCl_2$ and anti-CD2 mAb 12-15 (group X). (*a*) Marked and diffuse granular deposition of IgG (++++) in the glomerular mesangium, in the walls of arterioles, and in the basal part of tubular cells. (*b*) Dense deposits in the mesangial matrix. (*c* and *d*) Marked and diffuse granular deposition of IgG (++++) in the walls of alveolar capillaries (*c*) and in cardiac capillaries, myofibrils, and myofibril Z lines (*d*, *inset*). ×400 (*a*, *c*, and *d*); ×14,000 (*b*); ×700 (*d*, *inset*).

estingly, CTLA4 Rg failed to inhibit ongoing production of IL-4, consistent with observations by others (26) showing that CTLA4–Ig appears to have a pronounced blocking effect on Th1 responses but spares Th2-derived cytokines. Thus, it appears likely that other costimulatory pathways may be implicated in regulation of IL-4 production by T cells and that IL-4 production does not suffice to induce or maintain $HgCl_2$-associated autoimmune disease.

The effects of anti-CD2 mAbs RM2-1 and 12-15 have been extensively studied in vitro and in vivo. RM2-1 prevents CD2–CD48 interaction (8) and inhibits T cell activation (8, 24) whereas mAb 12-15 inhibits cytotoxic T cell

activity (10, 25) and suppresses contact sensitivity response (10, 11). Moreover, administration of mAb 12-15 prolongs allograft and xenograft survival by suppressing Th1 responses (12) and, when given in combination with anti-CD3 mAbs, anti–CD2 ligand (CD48) mAbs, or FK506, enables indefinite graft survival (13, 25). In contrast with their effects on Th1 activity, we found anti-CD2 mAbs RM2-1 and 12-15 to exacerbate $HgCl_2$-associated pathology in mice, resulting in marked increase in serum IgG, IgG1, IgE, and ANolAs; IL-4 production in the spleen; and transformation of a mild mesangial glomerulopathy into a severe systemic immune complex disease. Thus, these two anti-CD2 mAbs enhanced the $HgCl_2$-mediated Th2-dependent antibody response, reminiscent of their capacity to promote generation of $CD4^+$, IL-4–, and TGF-β–producing cells while suppressing cytotoxic T cell activity in vitro (25), and to stimulate the D10.G4.1 murine Th2 clone to produce IL-5, IL-6, and IL-10 (27).

Recent work has shown that antibodies directed at specific regions of the CD2 molecule can block T cell responsiveness to APC-derived IL-12 (28). Because IL-12 promotes naive $CD4^+$ cell differentiation to the Th1 phenotype and stimulates Th1 cell activity, engagement of CD2 results in suppression of Th1 cytokine production. Since Th1-derived cytokines inhibit Th2 function, suppression of Th1 activity may explain, in part, the observed increase in Th2-type responses. The effects of CD2 engagement, however, do not appear to be solely Th2 cytokine-dependent, since they are only partially attenuated by anti–IL-4 mAb and unaffected by anti–IL-10 mAb. Therefore, additional mechanisms, possibly cell contact dependent, may underlie the observed CD2-mediated stimulation.

The results of this study support the existence of a functional class of cell contact–dependent lymphocyte costimulatory pathways that determine whether any given helper T cell response will be of the Th1 or Th2 type. Thus, differentiation of Th cells toward the Th1 and Th2 phenotypes may be controlled by preferential interaction with B7.1- or B7.2-expressing APC (1), whereas CD2 derived signals may selectively regulate the effector functions of Th1 and Th2 cells, inhibiting Th1, while stimulating Th2 activity. The possibility of functionally manipulating these pathways offers potentially powerful approaches to the management of antibody-dependent autoimmune disease.

We thank Dr. Peter Altevogt for the anti-CD2 mAb 12-15 hybridoma and Drs. Reed and Coffman for gifts of the anti–IL-10 antibody.

This work was supported by National Institutes of Health grants CA-55735 and GM/AI-48614 to I. Stamenkovic and DK-36807 to G. Andres. I. Stamenkovic is a Scholar of the Leukemia Society of America. L. Biancone is recipient of the Dottorato di Ricerche in "Fisiopatologia dell' insufficienza renale," Cattedra di Nefrologia, Università di Parma.

Address correspondence to I. Stamenkovic, Department of Pathology, Harvard Medical School, and Pathology Research, Massachusetts General Hospital, 149 13th Street, Charlestown Navy Yard, Boston, MA 02129.

Received for publication 15 June 1995 and in revised form 5 December 1995.

References

1. Kuchroo, V.K., M. Prabhu Das, J.A. Brown, A.M. Ranger, S.S. Zamvil, R.A. Sobel, H.L. Weiner, N. Nabavi, and L.H. Glimcher. 1995. B7-1 and B7-2 costimulatory molecules activate differentially the Th1/Th2 developmental pathways: application to autoimmune disease therapy. *Cell.* 80:707–718.
2. Del Prete, G., E. Maggi, G. Pizzolo, and S. Romagnani. 1995. CD30, Th2 cytokines and HIV infection: a complex and fascinating link. *Immunol. Today.* 16:76–80.
3. Durie, F.H., T.M. Foy, S.R. Masters, J.D. Laman, and R.J. Noelle. 1994. The role of CD40 in the regulation of humoral and cell-mediated immunity. *Immunol. Today.* 15:406–411.
4. Linsley, P.S., P.M. Wallace, J. Johnson, M.G. Gibson, J.L. Greene, J.A. Ledbetter, C. Singh, and M.A. Tepper. 1992. Immunosuppression in vivo by a soluble form of the CTLA-4 T cell activation molecule. *Science (Wash. DC).* 257:792–795.
5. Linsley, P.S., W. Brady, L. Grosmaire, A. Aruffo, N.K. Damle, and J.A. Ledbetter. 1991. Binding of the B cell activation antigen B7 to CD28 costimulates T cell proliferation and interleukin 2 mRNA accumulation. *J. Exp. Med.* 173: 721–730.
6. De Boer, M., A. Kasran, J. Kwekkeboom, H. Walter, P. Vandenberghe, and J.L. Ceuppens. 1993. Ligation of B7 with CD28/CTLA-4 on T cells results in CD40 ligand expression, interleukin-4 secretion and efficient help for antibody production by B cells. *Eur. J. Immunol.* 23:3120–3125.
7. McArthur, J.G., and D.H. Raulet. 1993. CD28-induced costimulation of T helper type 2 cells mediated by induction of responsiveness to interleukin 4. *J. Exp. Med.* 178:1645–1653.
8. Kato, K., M. Koyanagi, H. Okada, T. Takanashi, Y.W. Wong, A.F. Williams, K. Okumura, and H. Yagita. 1992. CD48 is a counter-receptor for mouse CD2 and is involved in T cell activation. *J. Exp. Med.* 176:1241–1249.
9. Kanner, S.B., N.K. Damle, J. Blake, A. Aruffo, and J.A. Ledbetter. 1992. CD2/LFA-3 ligation induces phospholipase-C γ-1-tyrosine phosphorylation and regulates CD3 signaling. *J. Immunol.* 148:2023–2028.
10. Guckel, B., C. Berek, M. Lutz, P. Altevogt, V. Scirmacher, and B.A. Dyewski. 1991. Anti-CD2 antibodies induce T cell

unresponsiveness in vivo. *J. Exp. Med.* 174:957–967.
11. Bromberg, J.S., K.D. Chavin, P. Altevogt, B.A. Kyewski, B. Guckel, A. Naji, and C.F. Barker. 1991. Anti-CD2 monoclonal antibodies alter cell-mediated immunity *in vivo*. *Transplantation (Baltimore).* 51:219–225.
12. Chavin, K.D., H.T. Lau, and J.S. Bromberg. 1992. Prolongation of allograft and xenograft survival in mice by anti-CD2 monoclonal antibodies. *Transplantation (Baltimore).* 54:286–291.
13. Qin, L., K.D. Chavin, J. Lin, H. Yagita, and J.S. Bromberg. 1994. Anti-CD2 receptor and anti-CD2 ligand (CD48) antibodies synergize to prolong allograft survival. *J. Exp. Med.* 179:341–346.
14. Bigazzi, P.E. 1992. Lessons from animal models: the scope of mercury-induced autoimmunity. *Clin. Immunol. Immunopathol.* 65:81–84.
15. Goldman, M., P. Druet, and E. Gleichmann. 1991. Th2 cells in systemic autoimmunity: insights from allogeneic diseases and chemically-induced autoimmunity. *Immunol. Today.* 12: 223–227.
16. Ochel, M., H.W. Vohr, C. Pfeiffer, and E. Gleichmann. 1991. IL-4 is required for the IgE and IgG1 increase and IgG1 autoantibody formation in mice treated with mercuric chloride. *J. Immunol.* 146:3006–3011.
17. Bogen, S.A., I. Fogelman, and A.K. Abbas. 1993. Analysis of IL-2, IL-4, and IFN-γ producing cells *in situ* during immune responses to protein antigens. *J. Immunol.* 150:4197–4205.
18. Noelle, R.J., M. Roy, D.M. Shepherd, I. Stamenkovic, J.A. Ledbetter, and A. Aruffo. 1992. A 39-kDa protein on activated helper T cells binds CD40 and transduces the signal for cognate activation of B cells. *Proc. Natl. Acad. Sci. USA.* 89: 6550–6554.
19. Yagita, H., T. Nakamura, and K. Karasuyama. 1989. Monoclonal antibodies specific for murine CD2 reveal its presence on B as well as T cells. *Proc. Natl. Acad. Sci. USA.* 86:645–649.
20. Nishikawa, K., Y.-J. Guo, M. Miyasaka, T. Tamatani, A.B. Collins, M.-S. Sy, R.T. McCluskey, and G. Andres. 1993. Antibodies to intercellular adhesion molecule 1/lymphocyte function–associated antigen 1 prevent crescent formation in rat autoimmune glomerulonephritis. *J. Exp. Med.* 177:667–677.
21. Biancone, L., G. Andres, H. Ahn, C. DeMartino, and I. Stamenkovic. 1995. Inhibition of the CD40–CD40 ligand pathway prevents murine membranous glomerulonephritis. *Kidney Int.* 48:458–468.
22. Ohara, J., and W.E. Paul. 1985. Production of a monoclonal antibody to and molecular characterization of B cell stimulatory factor 1. *Nature (Lond.).* 315:333–336.
23. Mosmann, T., J. Schumacher, D. Fiorentino, J. Leverah, K. Moore, and M. Bond. 1990. Isolation of monoclonal antibodies specific for IL-4, IL-5, IL-6 and a new Th2-specific cytokine (IL-10), cytokine synthesis inhibitory factor, by using a solid phase radioimmunoadsorbent assay. *J. Immunol.* 145:2938–2942.
24. Ohno, H., T. Nakamura, H. Yagita, K. Okumura, M. Taniguchi, and T. Saito. 1991. Induction of negative signal through CD2 during antigen-specific T cell activation. *J. Immunol.* 147:2100–2106.
25. Chavin, K.D., L. Qin, R. Yon, J. Lin, H. Yagita, and J.S. Bromberg. 1994. Anti-CD2 mAbs suppress cytotoxic lymphocyte activity by the generation of the Th2 suppressor cells and receptor blockade. *J. Immunol.* 152:3729–3739.
26. Sayegh, M.H., E. Akalin, W.W. Hancock, M.E. Russell, C.B. Carpenter, P.S. Linsley, and L.A. Turka. 1995. CD28-B7 blockade after alloantigenic challenge in vivo inhibits Th1 cytokines but spares Th2. *J. Exp. Med.* 181:1869–1874.
27. Naora, H., J.G. Altin, and I.G. Young. 1994. TCR-dependent and -independent signaling mechanisms differentially regulate lymphokine gene expression in the murine T helper clone D10.G4.1. *J. Immunol.* 152:5691–5702.
28. Gollob, J.A., J. Li, E.L. Reinherz, and J. Ritz. 1995. CD2 regulates responsiveness of activated T cells to interleukin 12. *J. Exp. Med.* 182:721–731.